Acta Oceanol. Sin., 2015, Vol. 34, No. 1, P. 23–28
DOI: 10.1007/s13131-015-0592-0
http://www.hyxb.org.cn
E-mail: hyxbe@263.net

Spatial and temporal variation characteristics of ocean waves in the South China Sea during the boreal winter

ZHU Geli[1,3*], LIN Wantao[1], ZHAO Sen[1,2], CAO Yanhua[3]

[1] State Key Laboratory of Numerical Modeling for Atmospheric Sciences and Geophysical Fluid Dynamics, Institute of Atmospheric Physics, Chinese Academy of Sciences, Beijing 100029, China
[2] University of Chinese Academy of Sciences, Beijing 100049, China
[3] Department of Mathematics and Physics, North China Electric Power University, Beijing 102206, China

Received 9 April 2014; accepted 4 July 2014

Abstract

The spatial and temporal variation characteristics of the waves in the South China Sea (SCS) in the boreal winter during the period of 1979/1980–2011/2012 have been investigated based on the European Centre for Medium-range Weather Forecasts interim (ERA-Interim) reanalysis dataset. The results show that the leading mode of significant wave height anomalies (SWHA) in the SCS exhibits significant interannual variation and a decadal shift around the mid-1990s, and features a basin-wide pattern in the entire SCS with a center located in the west of the Luzon Strait. The decadal change from a weak regime to a strong regime is mainly associated with the enhancement of winter monsoon modulated by the Pacific decadal oscillation (PDO). The interannual variation of the SWHA has a significant negative correlation with the El Niño Southern Oscillation (ENSO) in the same season and the preceding autumn. For a better understanding of the physical mechanism between the SCS ocean waves and ENSO, further investigation is made by analyzing atmospheric circulation. The impact of the ENSO on the SWHA over the SCS is bridged by the East Asian winter monsoon and Pacific-East Asian teleconnection in the lower troposphere. During the El Niño (La Niña), the anomalous Philippine Sea anticyclone (cyclone) dominates over the Western North Pacific, helps to weaken (enhance) East Asian winter monsoon and then emerges the negative (positive) SWHA in the SCS.

Key words: ocean waves, interannual variability, South China Sea, ENSO, PDO

Citation: Zhu Geli, Lin Wantao, Zhao Sen, Cao Yanhua. 2015. Spatial and temporal variation characteristics of ocean waves in the South China Sea during the boreal winter. Acta Oceanologica Sinica, 34(1): 23–28, doi: 10.1007/s13131-015-0592-0

1 Introduction

The South China Sea (SCS) is the largest semi-enclosed marginal sea of the Pacific Ocean, located in the southernmost of Eurasia. The Taiwan Strait and the Luzon Strait in northeastern connect to the East China Sea and the western Philippine Sea. The Mindoro Strait in the east connects to the Sulu Sea, Sunda shelf in the southern SCS between the Malay Peninsula and Borneo exchanges water with Java Sea. The west boundary is adjacent to the Gulf of Tonkin, Vietnam and the Gulf of Thailand from north to south. The SCS has abundant resources, such as oil, gas, rare metals and fish. For these superior sea conditions, the SCS has become a busy shipping lane, and even been growing into a center of economic activities rapidly (Sharma et al., 1996), which provides a favorable environment to China's economic development.

The SCS is one of the most typical monsoon regions (Wyrtki, 1961), close to equatorial Pacific warm pool, influenced by the ascending branch of Walker circulation (Chen et al., 1997), local Hadley circulation and low-level cross-equatorial flows (Tan et al., 1995). The coastal areas in the SCS are frequently attacked by oceanic disasters that destroy people's lives and properties, thus, meteorological and oceanographic studies are urgently needed to ensure that human activity run on the rails. Ocean wave disaster, one of the most frequent marine disasters, has a deep social and economic influence on South China (Zhao et al., 2012). Investigating the ocean wave characteristics will help predict the ocean wave disaster and reduce the loss.

However, the ocean wave characteristics have not been well identified in the SCS due to lack of data before the 1980s. With the rapid development of satellite observations and data processing methods, more and more long-term datasets have been obtained for marine climate research (Chen et al., 2013). Many previous studies have shown that the ocean waves over the SCS have different timescale variations (Wang et al., 2001; Wang et al., 2003). For seasonal variations, Qi et al. (1997) firstly used monthly GEOSAT (GEOdetic SATellite) altimeter data to present that the significant wave height (SWH) in the SCS is stronger in the boreal winter than other seasons. Zhou et al. (2007) and Li et al. (2012) came to look for results based on ocean wave simulations in the SCS by using Wave Watch III wave model. For interannual variations, Guo et al. (2012) provided an evidence that wave height and surface wind variation are closely related to the Niño-3 index, and have a common period of 3–5 years that is consistent with the EI Niño-Southern Oscillation (ENSO) (Chen et al., 2006). Even so, the dynamic mechism between the SCS ocean wave variations and the ENSO has not been well identified.

In this work, we intend to study how the ENSO takes effect on the wave height in the SCS in the boreal winter. Few published studies have focused on the interdecadal varitions of the ocean

Foundation item: The National Basic Research Program (973 Program) of China under contract No. 2011CB403501.
*Corresponding author, E-mail: juliekxkl@126.com

waves in the SCS so far. This paper will give the interdecadal characteristic of the wave height and discuss its relationship with the Pacific decadal oscillation (PDO). Section 2 describes datasets and methods. Results are shown in Section 3, which includes typical anomalous significant wave height patterns in the SCS (Section 3.1), interdecadal variability (Section 3.2), and interannual variability (Section 3.3). Summary and conclusions are presented in Section 4.

2 Data and method

The ERA-Interim reanalysis dataset (Dee et al., 2011) with a resolution of 0.75°×0.75°during 1979–2012 provided by the European Centre for Medium-range Weather Forecasts (ECMWF) is used in this paper. For ocean wave observations, we use the fourth-daily significant height of combined wind waves and swell data (simply SWH hereafter) to produce monthly SWH data. Sorting the observed wave height in descending order, the average of the top one third wave height is called a significant wave height, it is an important variable which is widely used to study the ocean waves (Monaldo, 1988; Caires et al., 2004). For a wind field, we use a monthly mean wind at 10 m above the sea surface. Variable anomalies are defined as monthly mean departures from monthly climatology (1979–2012). The present study focuses on the boreal winter season (November, December, January, February and March, NDJFM).

The Niño3.4 index, defined as the sea surface temperature (SST) anomaly averaged within the region (5°N–5°S, 170°–120°W), is used to quantify the ENSO. The PDO is well known decadal variability of air-sea systems (Mantua and Hare, 2002), which is defined as the leading standardized principal component time series of monthly SST anomalies in the North Pacific (poleward of 20°N), with the global mean SST anomalies removed. The Niño3.4 index and the PDO index are downloaded from the Climate Prediction Center of the National Oceanic and Atmospheric Administration (NOAA) (http://www.esrl.noaa.gov/psd/data/climateindices/list/).

The methods used in this paper include empirical orthogonal function (EOF) analysis, regression analysis and composite analysis. The correlation coefficients corresponding to the 95% and 99% significance levels are 0.35 and 0.45, respectively, with a sample size of 32 (1979/1980–2011/2012).

3 Results

3.1 *Typical anomalous significant wave height patterns in the SCS*

In this section, the EOF analysis is applied to the monthly mean SWH anomalies (SWHA) to extract the dominant modes of variability over the winter SCS during 1979/1980–2011/2012 based on 6-hourly ERA-Interim reanalysis dataset. Figure 1 gives the two leading modes (EOF1 and EOF2) of the SWHA with a spatial distribution in the left panel and the corresponding normalized principal components (PC1 and PC2) in the right panel. The EOF1 and the EOF2 are well separated according to the criterion of North et al. (1982). They account for 78.4%, 9.2% of the total variance, respectively. The leading mode features a basin wide pattern in the whole SCS with a center located to the southwest of the Luzon Strait (17°N, 115°E). This center is also found by Chen et al. (2006), but their result is a little different from ours with the SWHA higher in the Taiwan Strait as well as the western Philippine Sea. In the positive phase of the normalized PC1 (Fig. 1), the basin-wide mode shows a higher SWHA in the western Philippine Sea along northeast and southwest and in the east of the Philippines. The PC1 exhibits significant interannual and decadal variabilities. The PC1 is strongly negative in 1982/1983, 1997/1998 and 2009/2010 which are precisely

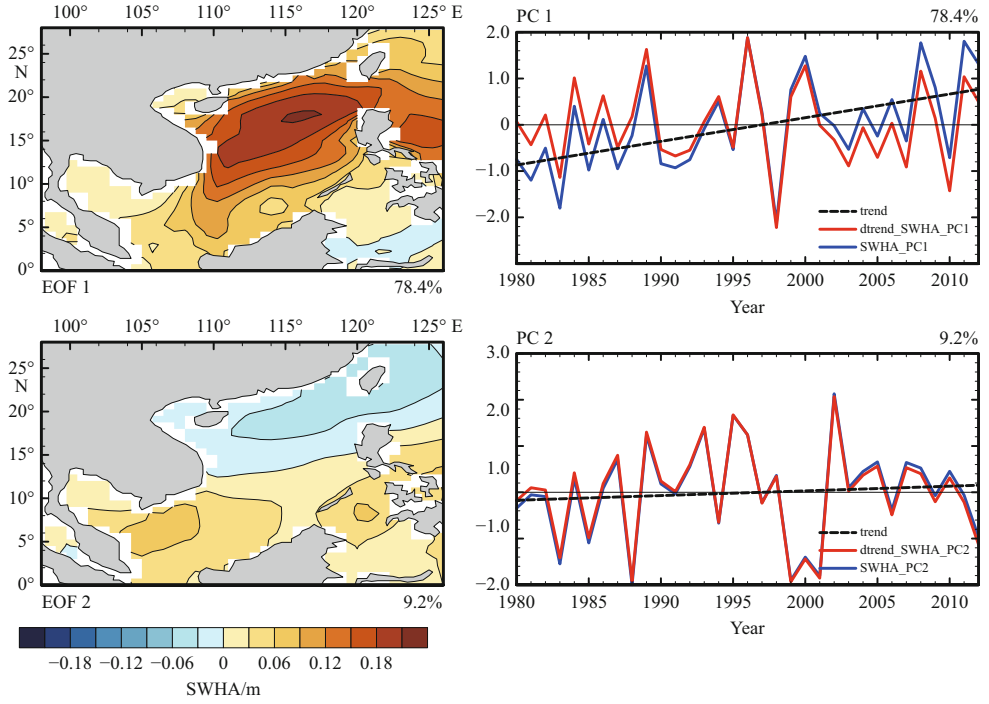

Fig. 1. The leading modes (EOF1 and EOF2, left panel) of significant wave height anomalies in the boreal winter during 1979/1980–2011/2012 and the corresponding normalized principal components (PC): PC1, PC2 (right panel). In the right panel, the blue, dashed and red lines denote the PC, the trend of the PC and the detrended PC, respectively. Explained variances are shown in the top-right corner of each subplot.

corresponding to the El Niño episodes in the eastern equatorial Pacific, meanwhile strongly positive in 1988/1989, 1995/1996, 1999/2000, 2008/2009 and 2010/2011 are corresponding to the La Niña episodes. Also the trend part of the PC1 is 0.05 m/year with a 99% significant level during the past 32 years from 1979/1980 to 2011/2012, indicating that the SWH is ascending with the PC1 phase shift in the mid-1990s (Fig. 1).

The EOF2 exhibits a meridional dipole mode with a node line located at about 13°N and no significant center on both sides. The trend part of the PC2 (dashed lines in PC2) is 0.01 m/year, which does not pass sinificant test at 50% level (*P*-value is equal to 0.40), indicating that interannual variation dominates the PC2. Hereafter we only show the result of the EOF1 because the higher mode explains total variance of the SWHA in the SCS.

The above analysis indicates that the PC1 has a phase shift in mid-1990s and is closely related to the ENSO. The decadal variations of the SWHA will be further discussed in Section 3.2. The analysis of the relationship between the ENSO and the SWHA in the SCS will be shown in Section 3.3.

3.2 *Interdecadal variability*

To reveal the interdecadal variability of the SWHA in the SCS, Figure 2 shows the averaged SWHA during 1979/80–1991/1992 (Fig. 2a) and 1999/2000–2011/2012 (Fig. 2b) and their difference (Fig. 2c). It is easy to see from Figs 2a and b that an opposite basin-wide SWHA signal exists in the SCS between 1979/80–1991/1992 and 1999/2000–2011/2012. The SWHA is stronger in the northern and central SCS (north of 10°N) than in the southern SCS (south of 10°N). Most area of the difference passes a statistical test at a confidence level of 99% (Fig. 2c), which implies that there indeed exists a decadal phase shift during 1979/1980–2011/2012 with a node year in the mid-1990s. These results are consistent with the EOF1 pattern and the PC1's time series as shown in Figs 1a and b, respectively.

The Pacific decadal oscillation (PDO) is widely regarded as a decadal variability with a phase shift from warm to cool during the late 1990s (Zhu et al., 2011), which has a great impact on the global climate. We are surprised to see the time of an interdecadal transformation is almost at the same period with that of the PC1 shift of the SWHA. To clarify whether exist the linkages between the phase shift of the SWHA in the SCS and the PDO, we compared the PDO in the boreal winter (NDJFM_PDO) and the preceding autumn (September, October, SO_PDO) with the PC1. The correlation coefficients between the SO_PDO and the PC1, the NDJFM_PDO and the PC1 are –0.53, –0.48, respectively. All the coefficients passed a significant test at 99% level which implies that the PDO in autumn/winter has impact on the SWHA in the SCS on decadal time-scale. Figure 3 only gives the PC1 of the SWHA and the preceding autumn PDO. Both of these time series exhibit a phase transition in the mid-1990s, with PDO averaged and PC1 averaged during 1979/1980–1991/1992 are 0.37, –0.55, respectively, and those during 1999/2000–2011/12 are –0.43, 0.50, respectively. Apparently, the SWH is below the normal condition in the SCS in the positive phase of the PDO. On the contrary, the SWHA is almost in the positive phase during the negative phase of the PDO.

What is the physical mechanism responsible for the phase shift of PDO in winter is not clear, a possible explanation is associated with the regional climate and the winter monsoon. Many efforts (Wang et al., 2008; Kim et al., 2014) have been made to explore the combined impacts of the ENSO and PDO on the East Asian winter monsoon. They have found that the La Niña occurs with a negative PDO phase that can lead to a robust East Asian winter monsoon. In contrast, the El Niño occurs with a positive PDO phase followed by a weakened East Asian winter monsoon. As we all know the anomalous monsoon will inevitably drive the ocean wave, and then modulate the variability of the SWH in the SCS. Hence, the imprint of the PDO phase shift signals in the mid-1990s on SWHA in the SCS can be attributed to the influence of the PDO on the East Asian winter monsoon.

3.3 *Interannual variability*

3.3.1 *Relationship between ENSO and SWH in the SCS*

The ENSO contains a strong signal in the atmosphere and ocean interaction that make a great difference to the interannual variability of the global atmospheric circulation (Torrence and Webster, 1998; Webster et al., 1998; He et al., 2008). The PC1 of the SWHA exhibits significant interannual fluctuation and strong anomaly years nearly coincide with the typical ENSO episodes. The above results indicate that the ENSO may have relationship between the interdecadal feature of the SWH in the SCS and the PDO in the boreal winter, so it is absolutely essential to reveal the links between ENSO events and SWHA variations in the SCS.

Figure 4 shows the detrended PC1 of the SWHA, the NDJFM mean Niño3.4 index, and the preceding autumn mean Niño3.4 index. To depict the interannual varibility of SWH perfectly, here we remove the trend of the PC1. Obviously, NDJFM mean Niño3.4 index are almost in the opposite phase with the detrended PC1. Namely, the positive (negitive) Niño3.4 index almost corresponds to the negitive (positive) phase of the detrended PC1, and vice versa. The correlation coefficient between the detrended PC1 and the Niño3.4 index is –0.79 in

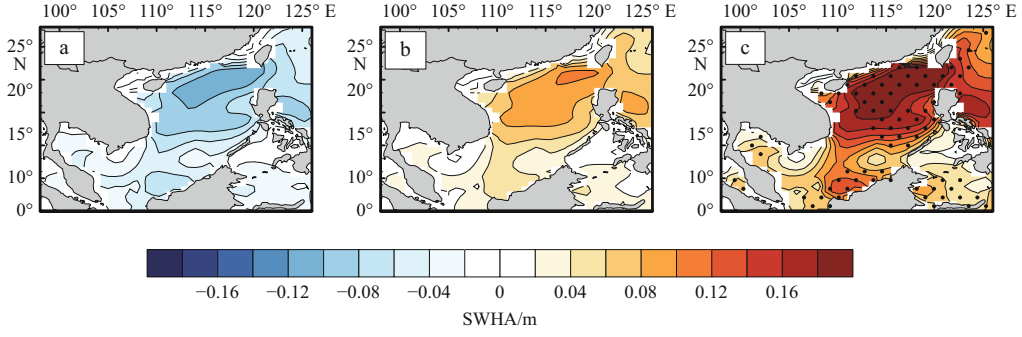

Fig. 2. Mean significant wave height anomalies in the boreal winter (NDJFM) during 1979/1980–1991/1992 (a) and 1999/2000-2011/2012 (b) and their differences (c). In Fig. 2c, dotted regions indicate significant values at a confidence level of 99% using a student's *t*-test.

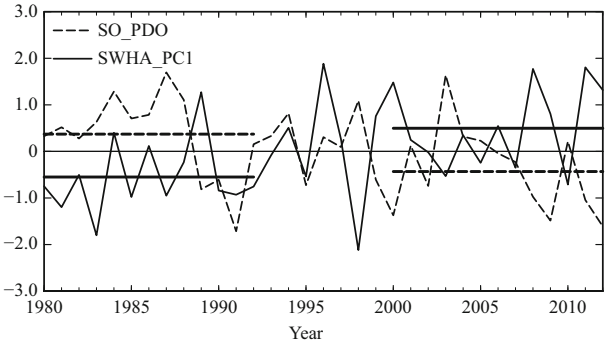

Fig. 3. The normalized PC1 of significant wave height (solid line) in the boreal winter during 1979/1980–2011/2012 and the PDO index in preceding autumn (dashed line), their averages during 1979/80–1991/1992 and 1999/2000–2011/2012 are horizontal lines.

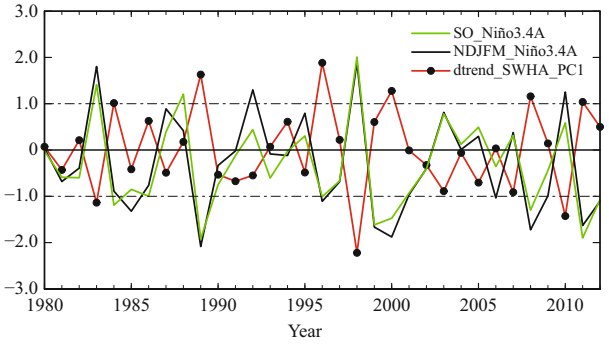

Fig. 4. The normalized NDJFM detrended PC1, NDJFM Niño-3.4 index, and the preceding autumn (SO) Niño-3.4 index during 1979/1980–2011/2012.

the synchronous season with a 99% significance level. And the detrended PC1 is also highly correlated with the preceding SO mean Niño3.4 index, whose correlation is –0.76 that pass 99% significance level. The aforementioned result also reveals that the ENSO in the preceding autumn may influence the SWH in the SCS in the boreal winter as the PDO.

Composite analysis is a common method for dealing with abnormal climate. We divided the strong ENSO years into El Niño year and La Niña year. The El Niño years (1983, 1987, 1992, 1995, 1998, 2003 and 2010) are defined as the standardized Niño3.4 index greater than 1.0, and the La Niña years (1985, 1989, 1999, 2000, 2008 and 2011) are defined as the standardized niño3.4 index less than –1.0. The composite SWHA during the El Niño years and the La Niña years aliased as the positive strong Niño3.4 (PSN) and the negative strong Niño3.4 (NSN) are shown in Figs 5a and b. The same way to find positive strong PC1 years (PSP: 1984, 1989, 1996, 2000, 2008 and 2011) and negtive strong PC1 years (NSP: 1983, 1998 and 2010), their corresponding spatial distributions of the composite SWHA are shown in Figs 5c and d any respectively.

For the composite years, the years in the PSP except 1984 and 1996 coincide with La Niña years, and the years in the NSP are all included in El Niño years. Therefore, the SWH in the SCS reserves tremendous information of the ENSO. During the El Niño years, the SWH is lower than that in normal years in the entire SCS basin. Conversely, SWHA is positive in the SCS during the La Niña years. That is along the lines of the earlier conclusion shown in Fig. 4. The four composite plots of the SWHA in the SCS shown in Fig. 5 exhibit a similar basin-wide spatial pattern along the northeast-southwest direction with a center located to the west of the Luzon Strait (15°–20°N, 113°–116°E). SWHA in composite PSP and NSN years are positive, while NSP and PSN years are negative. Correlation coefficients between any two of the four patterns are greater than 0.85. These all prove that the interannual modulation of the ENSO on the SWHA in the SCS is very important. The magnitudes of the SWHA in strong positive (negative) PC1 years are larger than those in La Niña (El Niño) years, which implies that the ENSO is not the only driving factor of interannual variations of the SWHA in the SCS in the boreal winter. The SWHA are relatively high in strong ENSO years than those in strong PC1 years to the southeast of the Luzon Strait in the Western Pacific, which may contribute to the SWHA in the SCS.

3.3.2 *Mechanism for how ENSO influencing SWH*

The above statistical analysis suggests that the leading mode of the SWHA in the SCS during the boreal winter is dominated by variations of preceding autumn and simultaneous ENSO signal. The physical mechanism for the impact of the ENSO on ocean waves in the SCS is not known yet. However, many studies have shown that the temporal and spatial variations of the SWH are closely associated with a local surface wind direction and speed (Wyrtki, 1961; Zhao et al., 2007; He and Wu, 2013). In particular, strong northeasterly winter monsoon winds prevailing over the whole SCS from November to March, meanwhile, the SCS is controlled by the northeastward waves.

The physical linkages between the ENSO and the East Asia winter monsoon have been investigated by many works (Tao and Zhang, 1998; Mu and Li, 1999; Chen, 2002; Ding et al., 2004; Wang et al., 2000), which formed a series of theories. A famous work by Wang et al. (2000) has interpreted the dynamic mechanism of the ENSO affecting East Asia monsoon, that is Pacific-East Asian teleconnection in the lower troposphere. The anomalous lower-tropospheric anticyclone (cyclone) located in the vicinity of the Philippine Sea is the key system that bridges the El Niño (La Niña) event in the equatorial eastern Pacific and weakens (strengthens) East Asian winter monsoons. Wang et al. (2000) implemented a model to show that the anomalous Philippine Sea anticyclone (cyclone) results from a Rossby wave response induced by local ocean surface cooling (warming) and central Pacific warming (cooling) when the El Niño (La Niña) event occurs, and persists because of the positive thermodynamic feedback between the local SST and anticyclone (cyclone) itself in the presence of mean northeasterly trades.

The regression map of the anomalous wind field in the SCS in the boreal winter on the Niño3.4 index multiplied by –1 is depicted in Fig. 6a. A typical anomalous cyclone dominates the larger part of the SCS that enhances northeasterly over the northern SCS, and the most area of the northern SCS (north of 15°N) passes 95% significance level. Meanwhile, the regressed wind field against with PC1 appears a similar anomalous cyclone and even the same significant region (Fig. 6b). The phenomenon can be explained by the Pacific-East Asian teleconnection theory. The anomalous cyclone circulation occurs near the Philippine Sea followed a cooling condition over the east equatorial Pacific, which will enhance the northeasterly over the northern SCS (Fig. 6c) and finally intensify the fluctuation ocean waves, increasing the SWH. In the same way, the anomalous anticyclone over northwestern Pacific is almost along with east equatorial Pacific warming event, and then controls the SWH in the SCS by affecting the wind field.

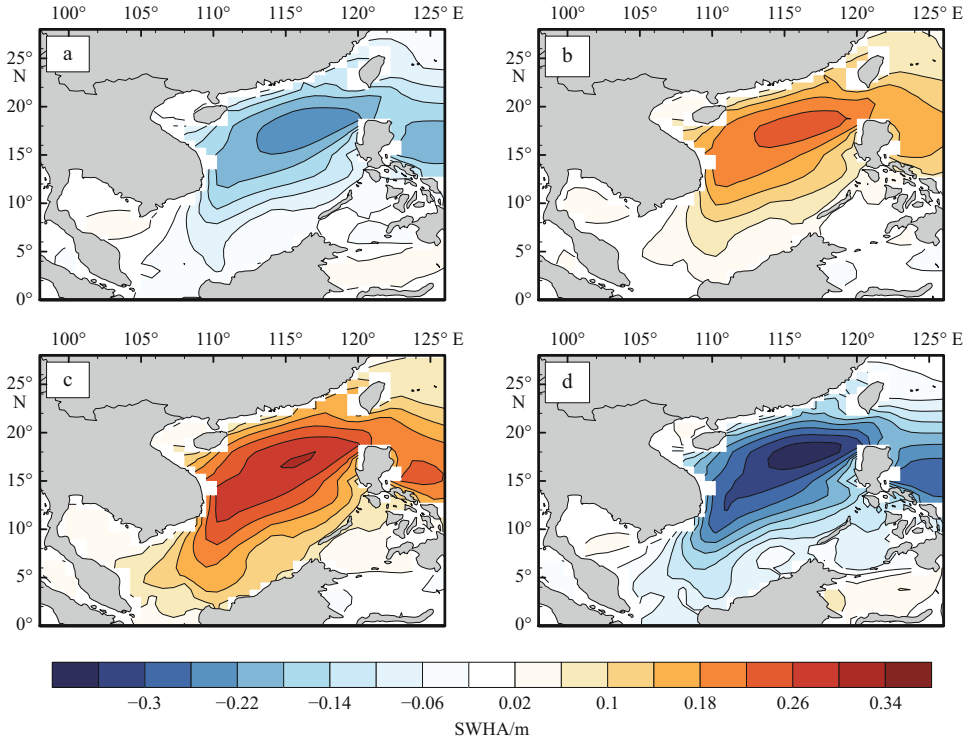

Fig. 5. Mean anomalous significant wave height in years with strong positive (a) and negative (b) ENSO, and strong positive (c) and negative (d) PC1 in the boreal winter in the South China Sea.

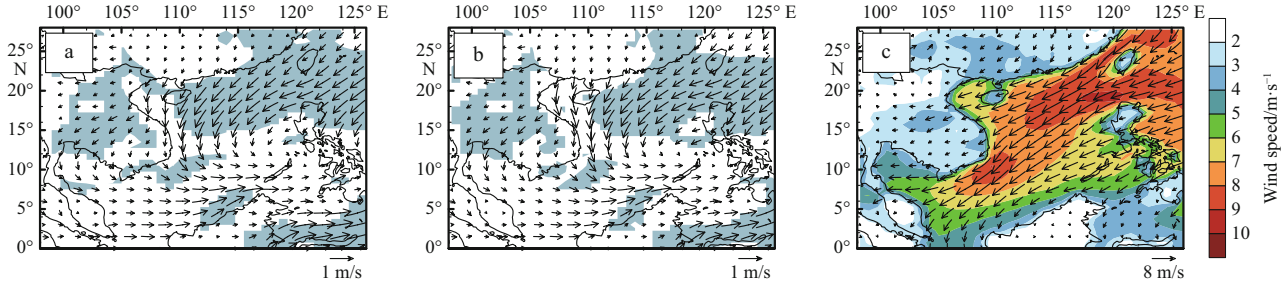

Fig. 6. Regression of surface wind (10 m) field against the normalized Niño-3.4 index multiplied by –1 (a) and NDJFM detrended PC1 (b). The shaded indicates significant values at a confidence level of 95%, and wind climatology (1979/1980–2011/2012) (c). In Fig. 6c, the colored denotes the wind speed.

4 Summary and discussion

In this paper, we investigated the temporal and spatial variations of the significant wave height in the SCS during the boreal winter (NDJFM) from 1979/1980 to 2011/2012 based on the high resolution ERA-Interim reanalysis dataset. The leading mode of the SWHA exhibits a basin-wide pattern in the entire SCS with a center located to the west of the Luzon Strait, explaining 78% of the total variance. The corresponding time series has remarkable interannual variations and a decadal shift in the mid-1990s from negative to positive.

The key of this work is to explore the relationship between the interannual variations of the NDJFM SWHA in the SCS and the ENSO. Analysis manifests that the SWHA variability is significantly negative correlated with the homochronous ENSO, especially in the strong ENSO years. We have attempted to document the dynamic mechanism of the ENSO affects the ocean waves variability in the SCS. Our results indicates the impact of the ENSO on the SWH in the SCS is bridged by the East Asian winter monsoon and the Pacific-East Asian teleconnection in the lower troposphere proposed by Wang et al. (2000). During the warm phase of the ENSO (El Niño), the anomalous anticyclone usually appears in the vicinity of Philippine Sea in the boreal winter, weakens the East Asian winter monsoon and leads to the SWH lower than the normal condition. Instead, for the cool phase of the ENSO (La Niña), anomalous cyclone covers the entire SCS, enhances the monsoon, increases the wave height and emerges the positive SWHA.

The decadal shift of the leading mode of the SWHA in the SCS is consistent with the PDO phase shift from warm to cool during the late 1990s, the same time period as the East Asia winter monsoon phase transportation (Zhu et al., 2011). Hence, we propose that PDO modulates the East Asia monsoon, and then conveys the decadal signal to ocean waves. Wang et al. (2008) presented that the impact of ENSO on East Asia winter monsoon can be modulated by PDO phase. Is there modulation of PDO on ENSO and ocean waves over the SCS? The problem is worth further study when long-term ocean waves data are available.

It should be note that the NDJFM SWH are also the closely correlated to the preceding autumn ENSO, which implies that the ENSO is potential predictor for the SWH in the SCS during the boreal winter in short-range climate prediction. The prediction model for the SWH in the SCS and their uncertainty analysis will be pursued in a subsequent publication.

Acknowledgements

The author would like to thank the anonymous reviewers for their constructive comments on the manuscript.

References

Caires S, Sterl A, Bidlot J R, et al. 2004. Intercomparison of different wind-wave reanalyses. Journal of Climate, 17(10): 1893–1913

Chen Yongli, Zhang Qinrong, Zhao Yongping. 1997. On the coupling oscillation between the Nansha warm water, the western Pacific subtropical high and ENSO. Studia Marina Sinica (in Chinese), 38(1): 87–97

Chen Chuntao, Zhu Jianhua, Lin Mingsen, et al. 2013. The validation of the significant wave height product of HY-2 altimeter-primary results. Acta Oceanologica Sinica, 32(11): 82–86

Chen Hongxia, Hua Feng, Yuan Yeli. 2006. Seasonal characteristics and temporal variations of ocean wave in the Chinese offshore waters and adjacent sea areas. Advances in Marine Science (in Chinese), 24(4): 407–415

Chen Wen. 2002. Impacts of El Niño and La Niña on the cycle of the East Asian winter and summer monsoon. Chinese Journal of Atmospheric Science, 26(5): 595–610

Dee D, Uppala S, Simmons A, et al. 2011. The ERA-Interim reanalysis: configuration and performance of the data assimilation system. Quart J Roy Meteor Soc, 137(656): 553–597

Ding Yihui, Li Chongyin, He Jinhai, et al. 2004. South China Sea monsoon experiment (SCSMEX) and East Asian summer monsoon. Acta Meteorologica Sinica (in Chinese), 20(2): 159–190

Guo Suiping, Zhuang Hui, Zheng Chongwei, et al. 2012. The relationship between El Niño and wave field in the South China Sea. Marine Forecasts (in Chinese), 29(6): 37–43

He Xicheng, Ding Yihui, He Jinhai. 2008. Response characteristics of the East Asian winter monsoon to ENSO events. Chinese Journal of Atmospheric Sciences (in Chinese), 32(2): 335–344

He Z Q, Wu R G. 2013. Coupled seasonal variability in the South China Sea. J Oceanogr, 69(1): 57–69

Kim J W, Yeh S W, Chang E C. 2014. Combined effect of El Niño-Southern Oscillation and Pacific decadal oscillation on the East Asian winter monsoon. Clim Dynam, 42(3–4): 957–971

Li Xunqiang, Zheng Chongwei, Su Qin, et al. 2012. Statistical analysis of wave and wind climate over China sea during 1988–2009. Journal of Ocean University of China (Natural Science) (in Chinese), 42(S1): 1–9

Mantua N J, Hare S R. 2002. The Pacific decadal oscillation. J Oceanogr, 58(1): 35–44

Monaldo F. 1988. Expected differences between buoy and radar altimeter estimates of wind speed and significant wave height and their implications on buoy-altimeter comparisons. Journal of Geophysical Research: Oceans (1978–2012) (in Chinese), 93(C3): 2285–2302

Mu Mingquan, Li Chongyin. 1999. ENSO signals in the interannual variability of East-Asian winter monsoon Part : Observed data analyses. Chinese Journal of Atmospheric Sciences, 23(3): 276–285

North G R, Bell T L, Cahalan R F, et al. 1982. Sampling errors in the estimation of empirical orthogonal functions. Mon Weather Rev, 110(7): 699–706

Qi Yiquan, Shi Ping, Mao Qinwen. 1997. Analysis on the seasonal mean characteristics of sea surface winds based on satellite remote sensing over the South China Sea. China offshore Platform, 12(03): 118–122

Sharma J N, Tryggestad S, Bian J. 1996. A comprehensive wind, wave and current measurement program in the South China Sea. Coastal Engineering Proceedings, 1(25): 354–367

Tan Jun, Zhou Faxiu, Hu Dunxin, et al. 1995. The correlation between SST anomaly in the South China Sea and ENSO. Oceanologia et Limnologia Sinica (in Chinese), 26(4): 377–382

Tao Shiyan, Zhang Qinyun. 1998. Response characteristics of the Asian winter and summer monsoon to ENSO events. Chinese Journal of Atmospheric Sciences, 22(4): 399–407

Torrence C, Webster P J. 1998. The annual cycle of persistence in the El Nino Southern Oscillation. Q J Roy Meteor Soc, 124(550): 1985–2004

Wang B, Wu R G, Fu X H. 2000. Pacific-East Asian teleconnection: how does ENSO affect East Asian climate? Journal of Climate, 13(9): 1517–1536

Wang L, Chen W, Huang R. 2008. Interdecadal modulation of PDO on the impact of ENSO on the East Asian winter monsoon. Geophys Res Lett, 35(20): 1–4

Wang Jing, Qi Yiquan, Shi Ping. 2001. Analysis on the characteristics of the sea surface wind and wave fields over the South China Sea using empirical orthogonal function. Haiyang Xuebao (in Chinese), 23(05): 136–140

Wang Jing, Qi Yiquan, Shi Ping, et al. 2003. Characteristics of sea surface height in South China Sea based on data from TOPEX/Poseidon. Journal of Tropical Oceanography, 22(04): 26–33

Webster P J, Magana V O, Palmer T N, et al. 1998. Monsoons: processes, predictability, and the prospects for prediction. J Geophys Res-Oceans, 103(C7): 14451–14510

Wyrtki K. 1961. Physical oceanography of the southeast Asia waters. In: Scientific Results of Marine investigations of the South China Sea and the Gulf of Thailand 1959–1961. NAGA Report 2. La Jolla, California: Scripps Institution of Oceanography, 195

Zhao Dongliang, Li Shuiqing, Song Chaoyang. 2012. The comparison of altimeter retrieval algorithms of the wind speed and the wave period. Acta Oceanologica Sinica, 31(3): 1–9

Zhao Wei, Tian Jiwei, Li Peiliang, et al. 2007. Effects of winds, tides and storm surges on ocean surface waves in the Sea of Japan. Acta Oceanologica Sinica, 26(3): 9–21

Zhou Liangming, Wu Lunyu, Guo Peifang, et al. 2007. Simulation and study of wave in South China Sea using WAVEWATCH-III. Journal of Tropical Oceanography, 26(5): 1–8

Zhu Yali, Wang Huijun J, Zhou Wen, et al. 2011. Recent changes in the summer precipitation pattern in East China and the background circulation. Clim Dynam, 36(7–8): 1463–1473